

TIME-HARMONIC FINITE ELEMENT SIMULATION OF A SHADED-POLE INDUCTION MACHINE

Herbert De Gersem and Kay Hameyer

Katholieke Universiteit Leuven, Dep. ESAT, Div. ELEN, Kasteelpark Arenberg 10, B-3001 Leuven-Heverlee, Belgium
E-mail: Herbert.DeGersem@esat.kuleuven.ac.be, Kay.Hameyer@esat.kuleuven.ac.be

Abstract

Elliptical air gap fields are decomposed by Fourier transforms into forward and backward rotating components. By applying these to two distinct rotor models, it is possible to account for motional eddy current effects by slip transformation. External circuit coupling and ferromagnetic saturation are considered. The overall approach simulates efficiently the steady-state behaviour of rotating shaded-pole induction machines without time stepping.

Introduction

To simulate a three-phase induction machine at steady-state, a time-harmonic finite element (FE) method can be used [1]. Motional eddy current effects are incorporated by *slip transformation*, i.e., by multiplying the rotor bar conductivities by the slip. The main assumption thereby is that the air gap field is a rotating, sinusoidal wave. In single-phase induction machines, however, the air gap field is alternating or, if an auxiliary winding or shading rings are applied, of an elliptical wave form (Fig. 1) [2]. Hence, time-harmonic simulation with slip transformation is no longer applicable. Existing simulation techniques are based on transient FE simulation [3], suffering from huge simulation times, or lumped parameter extraction methods, which may be inaccurate [4]. In this paper, a novel time-harmonic FE method with *air gap flux splitting* is presented and applied to a shaded-pole machine.

Single-Phase Induction Machine Model

The 2D time-harmonic magnetodynamic formulation is

$$-\frac{\partial}{\partial x} \left(v \frac{\partial \underline{A}_z}{\partial x} \right) - \frac{\partial}{\partial y} \left(v \frac{\partial \underline{A}_z}{\partial y} \right) + j\omega s \sigma \underline{A}_z = \frac{\sigma}{\ell_z} \underline{\Delta V} \quad (1)$$

with v the reluctivity, σ the conductivity, ω the electrical pulsation and ℓ_z the axial length of the 2D model [5]. The phasor \underline{A}_z corresponds to the z -component of the magnetic vector potential. The phasor $\underline{\Delta V}$ is the voltage drop between the front and rear ends of the model. The slip is defined by

$$s = \frac{\omega - \lambda \omega_m}{\omega} \quad (2)$$

with λ the pole pair number and ω_m the mechanical angular speed of the rotor. The slip represents the relative difference between the mechanical velocity and the speed of the rotating air gap wave ω/λ . The term $j\omega s \sigma \underline{A}_z$ accounts for both non-motional and motional eddy current effects. Slip transformation can be introduced by assigning the modified conductivity $\tilde{\sigma} = s\sigma$ to the moving conductors [6]. Discretising (1) on a triangulation of the 2D cross-section Ω , yields the system of equations $Ku = f$ with

$$K_{ij} = \int_{\Omega} \left(v \nabla N_i \cdot \nabla N_j + j\omega s \sigma N_i N_j \right) d\Omega; \quad f_i = \int_{\Omega} \frac{\sigma}{\ell_z} \underline{\Delta V} N_i d\Omega, \quad (3)$$

$N_j(x, y)$ the FE shape functions and u_j the associated degrees of freedom for \underline{A}_z . This formulation is not directly applicable to single-phase induction machines because in that case, the air gap field is not a true rotating wave and, hence, the configuration does not obey the necessary condition for slip transformation.

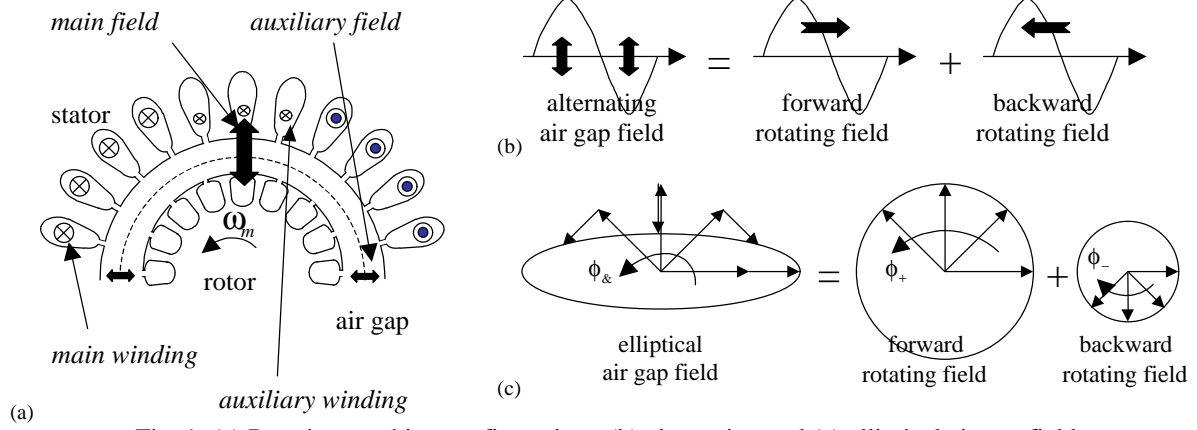


Fig. 1: (a) Rotating machine configuration ; (b) alternating and (c) elliptical air gap fields.

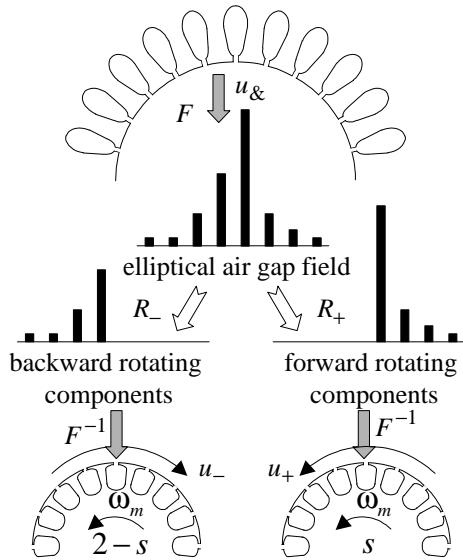


Fig. 2: Scheme of the air gap flux splitting approach.

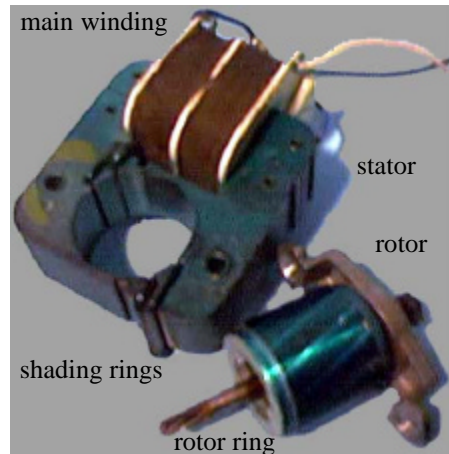


Fig. 3: Stator and rotor of the shaded-pole induction machine.

Analytical approaches for single-phase induction machines split the elliptical air gap field into two counter-wise rotating waves (Fig. 1). This idea is introduced in the time-harmonic FE formulation [7]. Three distinct models, one for the stator and two for the rotor, are considered (Fig. 2). They have a circular contour in the air gap in common. For notational convenience, assume three identical, equidistant FE grids at each of the matching boundaries. The vector of unknowns is partitioned by $u = (u_o \ u_{\&} \ u_+ \ u_-)$ with u_o the unknowns defined at FE nodes in the interior of the models and $u_{\&}$, u_+ and u_- those at the stator, first rotor and second rotor boundary respectively. The elliptical air gap field is decomposed into complex Fourier components: $c = Fu_{\&}$ with F the discrete Fourier transform. The positive harmonics $c_k, k > 0$ are propagated to the first rotor model, the negative harmonics $c_k, k \leq 0$ to the second rotor model. Hence, $u_+ = F^{-1}R_+c$ and $u_- = F^{-1}R_-c$ with R_+ and R_- , the operators selecting positive and negative harmonics respectively and $F^{-1} = F^H$ the inverse discrete Fourier transform.

The coupling of the disjoint models requires additional interface conditions. The continuity of the air gap flux corresponds to the constraints

$$\underbrace{\begin{bmatrix} 0 & R_+ F & F & 0 \\ 0 & R_- F & 0 & F \end{bmatrix}}_B u = \begin{bmatrix} 0 \\ 0 \end{bmatrix}. \quad (4)$$

The unknown tangential trace of the magnetic field strength in the air gap are represented by a set of Lagrange multipliers γ . Finally, a saddle-point formulation is achieved:

$$\begin{bmatrix} K & B^H \\ B & 0 \end{bmatrix} \begin{bmatrix} u \\ \gamma \end{bmatrix} = \begin{bmatrix} f \\ 0 \end{bmatrix}. \quad (5)$$

The system is solved by preconditioned Krylov subspace methods. Because these approach only requires the application of the system matrix and a preconditioner to a vector, the system matrix in (5) is not formed in practice [7]. Instead, explicit operators such as Fast Fourier Transforms (FFTs), inverse FFTs and appropriate selections are invoked for F , F^{-1} , R_+ and R_- .

If the original air gap field is elliptical, the magnetic field at the boundary of each rotor model is a sinusoidal, rotating magnetic wave. Therefore, it is possible to account for motional eddy current effects by slip transformation in each rotor model independently. The first rotor model experiences an air gap field rotating at the angular velocity ω/λ . The slip of the rotating conductors with respect to this wave is $s_+ = s$. The air gap field incident to the second rotor model rotates at $-\omega/\lambda$ and gives rise to the slip $s_- = 2 - s$. Motional eddy currents are correctly taken into account by applying the modified conductivities $\tilde{\sigma}_+ = s\sigma$ and $\tilde{\sigma}_- = (2 - s)\sigma$ to the first and second rotor models respectively. If the stator or rotor is slotted, this technique applies approximately. Based on the satisfactory results for technical three-phase induction machines, however, it is expected that this approach is sufficiently accurate for a large class of single-phase designs. This approach has substantial advantages over the transient simulation. It enables the steady-state simulation of single-phase induction machines accounting for motional eddy currents but without time-stepping or moving the meshes. Therefore, the method is extremely fast and applicable within design procedures and optimisation routines.

For technical models, 3D effects can not be neglected [6]. The winding, shading rings and rotor bars are connected to an external circuit with lumped parameters representing the voltage source and the additional resistance and inductance of the parts of the winding, shading rings and rotor bars outside the 2D model (Fig. 4). The air gap flux splitting approach gives rise to two disjoint external circuits modelling the squirrel cage. The end ring resistances have to be scaled according to the different slip values [6]. For computational efficiency, it is recommended to embed the circuit equations in (5) using the approach described in [8].

The air gap flux splitting is a particular application of superposition. To consider non-linear materials, an iterative procedure has to be set up. Intermediate solutions are constructed on a third rotor model (in the figures positioned within the stator) by summing up the contributions of both rotor models. New permeabilities are determined and distributed back to the separate rotor models before the next step in the non-linear iteration.

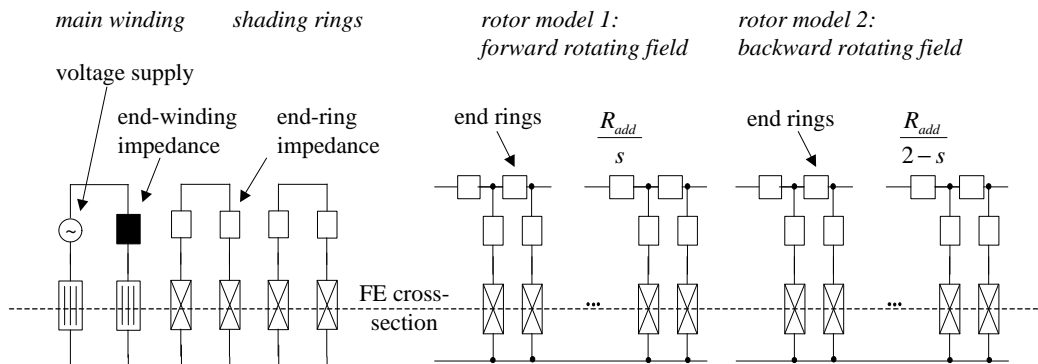


Fig. 4: External circuit connecting the stranded and solid conductors to impedances, modelling end-windings and end-rings, and to the voltage supply.

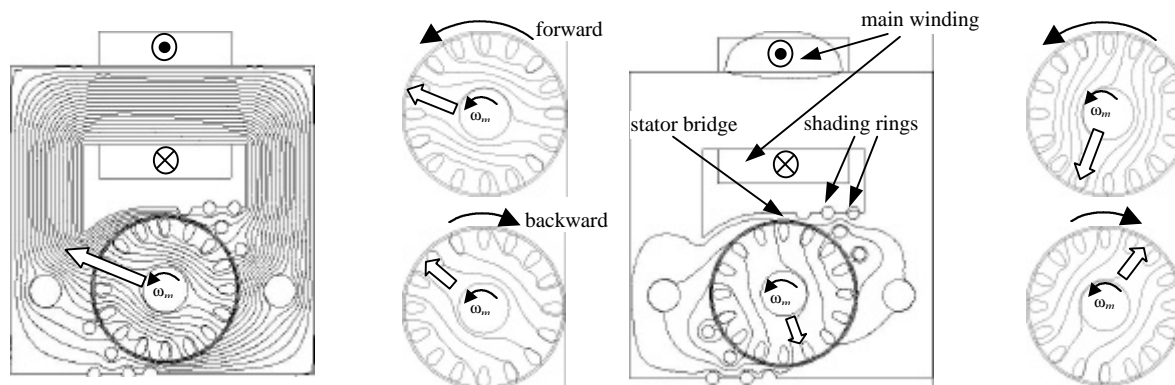


Fig. 5: Magnetic flux lines in a shaded-pole machine at t_0 and t_1 , shifted over 90° electrically in time (the block arrows indicate flux vectors).

Application: Shaded-Pole Induction Machine

In Fig. 5, the magnetic flux in a shaded-pole machine is plotted at two instants t_0 and t_1 , one quarter of a period shifted in time. The rotor within the stator reflects the overall solution. In the two separate rotor models, an electrical shift of 90° corresponds to a mechanical shift of 90° , indicating the rotation of the fields. Because of the shading rings, the air gap field is elliptical and the revolving fields have a slightly different magnitude. The stator bridges experience substantial saturation. The external circuit shown in Fig. 4 models the 3D effects and the voltage supply. The time-harmonic approach with air gap flux splitting and slip transformation enables the steady-state simulation of shaded-pole machine in a few minutes of computation whereas a transient approach achieving the same accuracy takes more than a day.

Conclusions

The combination of the novel air gap flux splitting approach and slip transformation constitutes a convenient and efficient time-harmonic finite element simulation of shaded-pole induction machines operated at steady-state.

Acknowledgement

The authors are grateful to the Belgian "Fonds voor Wetenschappelijk Onderzoek Vlaanderen" (project G.0427), the Belgian Ministry of Scientific Research (IUAP No. P4/20 on Coupled Problems in Electromagnetic Systems) and the Research Council of the Katholieke Univeriteit Leuven for the financial support of this work.

References

- [1] E. Vassent, G. Meunier and J.C. Sabonadière, Simulation of induction machine operation using complex magnetodynamic finite elements, *IEEE Transactions on Magnetics*, Vol. 25, No. 4, 1989, pp. 3064-3066.
- [2] H.-D. Stölting and A. Beisse, *Elektrische Kleinmaschinen*, B.G. Teubner, Stuttgart, 1987.
- [3] N. Sadowski, R. Carlson, S.R. Arruda, C.A. da Silva and M. Lajoie-Mazenc, Simulation of single-phase induction motor by a general method coupling field and circuit equations, *IEEE Transactions on Magnetics*, Vol. 31, No. 3, 1995, pp. 1908-1911.
- [4] S. Williamson and A.C. Smith, A unified approach to the analysis of single-phase induction motors, *IEEE Transactions on Industry Applications*, Vol. 35, No. 4, 1999, pp. 837-843.
- [5] P.P. Silvester and R.L. Ferrari, *Finite Elements for Electrical Engineers*, 2nd ed, Cambridge University Press, Cambridge, 1996.
- [6] R. De Weerd, E. Tuinman, K. Hameyer and R. Belmans, Finite element analysis of steady state behavior of squirrel cage induction motors compared with measurements, *IEEE Transactions on Magnetics*, Vol. 33, No. 2, 1997, pp. 2093-2096.
- [7] H. De Gerssem and K. Hameyer, Air gap flux splitting approach for single-phase induction machines, submitted to *Compumag*, Evian, 7-11 July 2001.
- [8] H. De Gerssem, R. Mertens, U. Pahner, R. Belmans and K. Hameyer, A topological method used for field-circuit coupling, *IEEE Transactions on Magnetics*, Vol. 34, No. 5, 1998, pp. 3190-3193.